

# On the Construction of Diabatic and Adiabatic Potential Energy Surfaces Based on Ab Initio Valence Bond Theory<sup>†</sup>

Lingchun Song\* and Jiali Gao\*

Department of Chemistry and the Minnesota Supercomputing Institute, Digital Technology Center, University of Minnesota, Minneapolis, Minnesota 55455

Received: April 8, 2008; Revised Manuscript Received: July 4, 2008

A theoretical model is presented for deriving effective diabatic states based on ab initio valence bond self-consistent field (VBSCF) theory by reducing the multiconfigurational VB Hamiltonian into an effective two-state model. We describe two computational approaches for the optimization of the effective diabatic configurations, resulting in two ways of interpreting such effective diabatic states. In the variational diabatic configuration (VDC) method, the energies of the diabatic states are variationally minimized. In the consistent diabatic configuration (CDC) method, both the configuration coefficients and orbital coefficients are simultaneously optimized to minimize the adiabatic ground-state energy in VBSCF calculations. In addition, we describe a mixed molecular orbital and valence bond (MOVB) approach to construct the CDC diabatic and adiabatic states for a chemical reaction. Note that the VDC-MOVB method has been described previously. Employing the symmetric  $S_N2$  reaction between  $NH_3$  and  $CH_3NH_3^+$  as a test system, we found that the results from ab initio VBSCF and from ab initio MOVB calculations using the same basis set are in good agreement, suggesting that the computationally efficient MOVB method is a reasonable model for VB simulations of condensed phase reactions. The results indicate that CDC and VDC diabatic states converge, respectively, to covalent and ionic states as the molecular geometries are distorted from the minimum of the respective diabatic state along the reaction coordinate. Furthermore, the resonance energy that stabilizes the energy of crossing between the two diabatic states, resulting in the transition state of the adiabatic ground-state reaction, has a strong dependence on the overlap integral between the two diabatic states and is a function of both the exchange integral and the total diabatic ground-state energy.

## 1. Introduction

The concept of effective valence bond (VB) theory introduced by Sason Shaik has profoundly influenced our understanding of the structure and reactivity of chemical reactions.<sup>1–3</sup> In this theory, the reactant and product states as well as other Lewis resonance structures are represented by effective diabatic states, which are then coupled to yield the adiabatic potential energy surface, avoiding crossing between diabatic states.<sup>2</sup> However, until recently, it has been difficult to obtain accurate energies of these effective VB states.<sup>4–11</sup> In fact, there is great interest to extend these ideas to study chemical reactions quantitatively in solution and in enzymes.<sup>4–10,12–22</sup> In this paper, we present a theoretical approach for constructing such effective diabatic states and computing the adiabatic ground-state energy.

Ab initio valence bond (VB) theory is clearly the most appropriate method for understanding effective diabatic states;<sup>23–28</sup> however, the large number of VB configurations involved make it both qualitatively cumbersome in interpretation and quantitatively intractable in computation, especially for large and condensed phase systems. Alternatively, we have developed a mixed molecular orbital and valence bond (MOVB) theory,<sup>4,5</sup> in which effective diabatic states are constructed by a block-localized wave function (BLW) method.<sup>29–36</sup> In the BLW model, molecular orbitals (MOs) are strictly localized according to the specific Lewis resonance structure. These localized MOs possess key features as in VB theory such that MOs in different charge-

localization blocks are nonorthogonal, whereas MOs in the same fragment are orthogonal.<sup>29–32</sup> Furthermore, because molecular orbitals are delocalized within a given block (fragment) of localization, the large number of valence bond configurations in VB theory is reduced to just a single MOVB states, which can be used to form an effective valence bond Hamiltonian. The MOVB method has been applied to a number of reactions in solution by means of combined quantum mechanical and molecular mechanical (QM/MM) simulations.<sup>4,5,13,14</sup>

The aim of this paper is to develop a theoretical basis for deriving the effective diabatic states from ab initio valence bond self-consistent field (VBSCF)<sup>27,37,38</sup> theory by systematically reducing the multiconfigurational VB Hamiltonian into an effective two-state model. Our present interest is on atom- and group-transfer reactions, such as nucleophilic displacement ( $S_N2$ ) and proton-transfer reactions and the method is general in these applications; it is possible that there are cases where the reactant and product states cannot be immediately written in terms of valence bond configurations. In this case, further research is needed to generalize the present work in specific applications. This theoretical result is then used to compare with and to validate the MOVB method. Furthermore, we present two computational approaches to construct the diabatic states. The first is called the variational diabatic configuration MOVB (VDC-MOVB) in which the individual energies of diabatic states are variationally minimized, and then used in configuration interaction calculations to obtain the energy of the adiabatic ground state. The second approach is termed as consistent diabatic configuration MOVB (CDC-MOVB), in which both

<sup>†</sup> Part of the "Sason S. Shaik Festschrift".

\* Address correspondence to Lingchun Song (songx184@umn.edu) or Jiali Gao (jgao@umn.edu).

the configuration coefficients and orbital coefficients are simultaneously optimized to minimize the adiabatic ground-state energy. These two variational approaches are also incorporated into VBSCF calculations, and used to validate the MOVb results. This comparison also paves a way for systematically deriving and optimizing an effective Hamiltonian MOVb (EH-MOVb) method for modeling chemical reactions. We use the symmetric  $S_N2$  reaction of  $H_3N + CH_3NH_3^+$  to illustrate the computational procedure.

In the following, we first present the theory to systematically reduce ab initio valence bond configurations into a two-effective-state model for nucleophilic substitution reactions. Then, the mixed molecular orbital and valence bond (MOVb) theory is reviewed, followed by a summary of computational details. Results and discussions are presented next. Finally, the paper concludes with a summary of the major findings of this study and future perspectives.

## 2. Definition of Effective Diabatic States Based on Valence Bond Theory

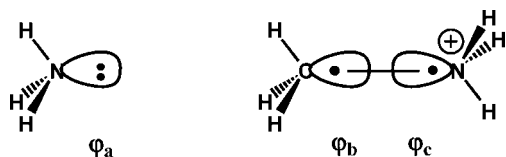
In valence bond theory,<sup>23,26,39</sup> the ground-state wave function  $\Phi$  for a molecular system is written as a linear combination of all VB-state configurations  $\{\Psi_K; K = 1, \dots, N\}$ : resulting from  $N$  possible ways of distributing the “active” electrons into the “active” orbitals (see below)

$$\Phi = \sum_K a_K \Psi_K \quad (1)$$

where  $\Psi_K$  is a Heitler–London–Slater–Pauling (HLSP) function or its equivalent form, and  $a_K$  is the coefficient for state  $K$ .

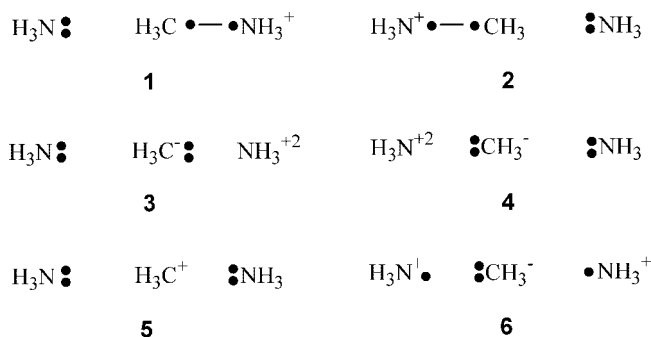
Two types of ab initio VB computations are typically performed. In the self-consistent field valence bond (VBSCF) method,<sup>27,37,38</sup> both the state coefficients in eq 1 and orbital coefficients of each VB structure are simultaneously optimized to yield the minimum energy of the system. Note that in VBSCF, the VB orbitals are the same for all configurations. The VBSCF result is comparable to that from complete active space self-consistent field (CASSCF) calculations in molecular orbital theory,<sup>40</sup> which includes static electron correlation effects. In the second approach, in which dynamic correlation effects are partially included, the basis orbitals are more flexible and allowed to vary in different VB configurations. Thus, this breathing orbital valence bond (BOVB) method allows the orbitals to respond to the electric field of the individual VB configurations as opposed to the average field of all VB states in the VBSCF approach.<sup>9,10,26,41</sup> In principle, BOVB can yield more accurate results than standard VBSCF calculations.

For the symmetric  $S_N2$  reaction between  $H_3N$  and  $H_3C-NH_3^+$ , there are four “active electron” in the VB treatment, two from the lone pair of the nucleophile ( $H_3N:$ ) and two from the chemical bond between the substrate carbon and the leaving group ( $H_3C-NH_3^+$ ), and there are three orbitals to form the “active space”, one from each of the three fragments, including the nucleophile ( $\varphi_a$ ), the leaving group ( $\varphi_c$ ) and the substrate



( $\varphi_b$ ). Of this active space, there are a total of 6 ways of arranging four electrons in three orbitals, which constitute the six

## SCHEME 1: Schematic Representation of the Valence Bond Structures for the $S_N2$ Reaction between $H_3N$ and $CH_3NH_3^+$



fundamental VB structures (Scheme 1) to form the ground-state VB wave function. Specifically, the individual VB structures are defined as follows:

$$\Psi_1 = \hat{A} \{ \Omega_c ({}^2\varphi_a) \varphi_b \varphi_c (\alpha\beta - \beta\alpha) \} \quad (2a)$$

$$\Psi_2 = \hat{A} \{ \Omega_c ({}^2\varphi_c) \varphi_a \varphi_b (\alpha\beta - \beta\alpha) \} \quad (2b)$$

$$\Psi_3 = \hat{A} \{ \Omega_c ({}^2\varphi_a) ({}^2\varphi_b) \} \quad (2c)$$

$$\Psi_4 = \hat{A} \{ \Omega_c ({}^2\varphi_b) ({}^2\varphi_c) \} \quad (2d)$$

$$\Psi_5 = \hat{A} \{ \Omega_c ({}^2\varphi_a) ({}^2\varphi_c) \} \quad (2e)$$

$$\Psi_6 = \hat{A} \{ \Omega_c ({}^2\varphi_b) \varphi_a \varphi_c (\alpha\beta - \beta\alpha) \} \quad (2f)$$

where  $\hat{A}$  is an antisymmetrizing operator,  $\Omega_c$  is the product of all remaining occupied orbitals not included in the VB active space,  $\alpha$  and  $\beta$  are electron spin orbitals, and  $({}^2\varphi_\mu)$  denotes double occupation of the VB orbital  $\varphi_\mu$ . In Scheme 1, states 1 and 2 are the covalent Heitler–London structures for the reactant and product state, respectively, each of which uses two Slater determinants to describe the spin-pairing interactions in the corresponding single bond.<sup>42</sup> The ionic configurations for the C–N bond in either the reactant or the product states are specified by structures 3 and 5, and structures 4 and 6, respectively. Finally, configuration 6 describes the spin pairing between the two electrons localized on the nucleophile and leaving group with the substrate central carbon orbital doubly occupied.

Of particular interest are the two limiting regions at the reactant state and the product state.<sup>2,3</sup> For the reactant state ( $R$ ), where the nucleophile, ammonia, and the substrate, methylammonium ion, are fully separated, its wave function  $\Phi^R$  is the mixture of the Heitler–London covalent configuration  $\Psi_1$  and the two ionic states  $\Psi_3$  and  $\Psi_5$ , which correspond to the description of the Lewis resonance structure for the C–N bond of the substrate with the nucleophile  $H_3N$  acting as a spectator.

$$\Phi^R = c_1^R \Psi_1 + c_3^R \Psi_3 + c_5^R \Psi_5 \quad (3)$$

Similarly, for the product state ( $P$ ), the wave function  $\Phi^P$  is a linear combination of the covalent-state  $\Psi_2$  and the ionic states of  $\Psi_4$  and  $\Psi_5$ :

$$\Phi^P = c_2^P \Psi_2 + c_4^P \Psi_4 + c_5^P \Psi_5 \quad (4)$$

The wave functions defined by eqs 3 and 4 describe the Lewis bond states for the reactant and product, respectively. It is important to note that both the reactant and product states share the key ionic structure,  $\Psi_5$ .

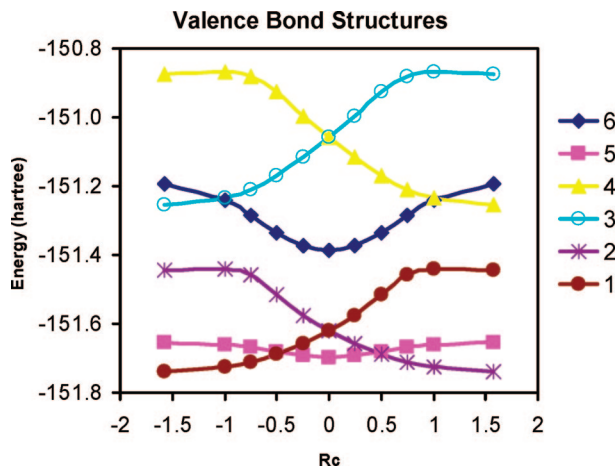


**Figure 1.** Energy profiles of valence bond structures along the reaction coordinate for the  $S_N2$  reaction of  $H_3N$  and  $CH_3NH_3^+$ . Energies are given in hartrees, and the reaction coordinate is defined as the difference between the distances of the breaking and forming bonds in angstroms. The individual VB configurations are labeled in accordance with the structures depicted in Scheme 1.

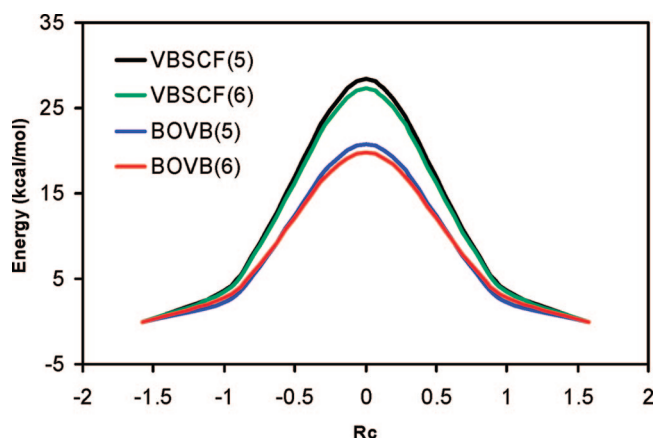


**Figure 2.** Relative ground-state potential energies (kcal/mol) for the reaction between  $H_3N$  and  $CH_3NH_3^+$  along the reaction coordinate, determined by using VBSCF and BOVB theory with six and five valence bond structures, the latter of which excludes VB structure **6** in Scheme 1. The reaction coordinate is given in angstroms.

The “outer” spin-pairing configuration,  $\Psi_6$ , corresponds to a charge-transfer excited state that does not contribute to the Lewis structure of the respective C–N bond in the reactant and the product state. However, it interacts and further stabilizes the adiabatic ground state. In Shaik’s original VB correlation approach,<sup>2</sup> the reactant Lewis structure correlates with the charge-transfer excited state of the product configuration, and the product Lewis structure correlates with that of the reactant state. At the transition state, where the three fragments involved in the bond forming and breaking process have the most compact geometry along the reaction coordinate, configuration **6**,  $\Psi_6$ , makes the greatest contribution to the molecular wave function (Figure 1). Nevertheless, its effect in lowering the overall reaction barrier is still rather small in the present  $S_N2$  reaction, as shown in Figure 2, from both VBSCF and BOVB calculations. Consequently, we have decided to utilize the pure Lewis bond configurations, eqs 3 and 4, in the following analysis without sacrificing accuracy and generality. We emphasize, however, that it is straightforward to include  $\Psi_6$  in eqs 3 and 4, just as the inclusion of the shared-state  $\Psi_5$ .

Clearly, eqs 3 and 4 (and the extension to include  $\Psi_6$ ) provide a well-defined method for a two-state model on the basis of ab

initio valence bond theory, and these two states are called effective diabatic states, corresponding to the reactant and product states, respectively. They are effective states because the two-state model has been deduced from all of the VB configurations, which can be used to reproduce exactly the adiabatic ground-state energy of the original ab initio VB theory.

To describe the change in energy and wave function of the two Lewis bond states as the reaction takes place, we define the reaction coordinate here as the difference between the bond length of the central carbon and the leaving group  $R(C-N_P)$  and that of the nucleophile and the central carbon  $R(C-N_R)$ :

$$R_c = R(C-N_P) - R(C-N_R) \quad (5)$$

Of course, one can use other definitions to monitor the progress of the reaction, including the difference between the corresponding bond orders or energies of the two Lewis bond states. The geometrical variable, corresponding to the asymmetric bond stretch coordinate, is a good choice and of chemically intuitive. In Shaik’s VB correlation diagram,<sup>2</sup> the mixing or resonance of the two Lewis structures,  $\Phi^R$  and  $\Phi^P$ , avoids crossing between the two states, resulting in the transition state and an adiabatic ground-state potential surface along the entire reaction coordinate.

### 3. Effective Two-State Valence Bond Model

In this section, we aim at constructing a two-state VB theory that can be used in effective Hamiltonian<sup>43</sup> VB (EHVB) calculations based on the two-state diabatic configurations defined in eqs 3 and 4. This EHVB model can be used to study chemical reactions in solution,<sup>4,5,14</sup> and it can be used to validate the MOVVB effective diabatic states discussed in the following section. We present two ways of optimizing the effective diabatic states, both of which are well-defined on the basis of variational principle, although they result in different quantitative values and qualitative interpretations. In the first approach, we deduce the diabatic states directly from the VB configurations that optimize the ground-state energy in VBSCF calculations. Thus, they are called consistent diabatic configurations (CDC). In the second approach, the diabatic states are determined independently by minimizing the energies of the individual wave functions in eqs 3 and 4. These states are called variational diabatic configurations (VDC). The effective Hamiltonian, using either CDC or VDC states, can be constructed to reproduce exactly the ground-state energy from VBSCF theory.

**3.1. Consistent Diabatic Configuration.** Having defined the effective diabatic state as the corresponding Lewis bond configuration for the reactant and product, which can be further decorated by charge-transfer excited states,<sup>2,3</sup> we present a formulation to determine the specific VB coefficients in eqs 3 and 4 and the resonance integral in the context of the two-state VB effective Hamiltonian. We begin with the secular equation employing the diabatic states of eqs 3 and 4 as the basis set:

$$\begin{vmatrix} H_{11}^{CDC} - \varepsilon & H_{12}^{CDC} - \varepsilon S_{12}^{CDC} \\ H_{21}^{CDC} - \varepsilon S_{21}^{CDC} & H_{22}^{CDC} - \varepsilon \end{vmatrix} = 0 \quad (6)$$

where the superscript specifies the CDC effective diabatic state,  $\varepsilon$  is the adiabatic potential energy,  $H_{ij}^{CDC}$  is a Hamiltonian matrix element and  $S_{12}^{CDC} = S_{21}^{CDC}$  is the overlap integral between the two effective states. In the CDC-VBSCF model, the orbital and VB configurational coefficients are derived directly from VBSCF theory. Thus, the configuration coefficients of states **1** and **3** for the reactant diabatic state in eq 3, and those of states **2** and **4** for the product state in eq 4, are uniquely defined and identical to the corresponding VBSCF values because they do



not contribute to the Lewis structure of the other state. Thus, we have these diabatic-state coefficients expressed in terms of the VBSCF configuration coefficients as follows

$$c_1^R = a_1 \quad c_3^R = a_3 \quad (7)$$

and

$$c_2^P = a_2 \quad c_4^P = a_4 \quad (8)$$

The ionic structure **5**, however, is shared by both diabatic states, and its VBSCF configuration coefficient must be divided between the two effective diabatic states. More importantly, this division must be dependent on molecular structure, which results in different charge polarization along the reaction coordinate. Examination of the configuration weight of structure **5** in the VBSCF ground state indicates that it has the smallest contributions in both the reactant and product structures and the largest component at the transition state (Figure 1).<sup>10</sup> This trend is consistent with and can be related to the partial charge on the central carbon as noted previously by Song et al. in their study of the identity  $S_N2$  reactions involving halogen ions.<sup>9,10</sup> In fact, there are many different ways of representing the partition of structure **5** into the two diabatic states, which means that there are also many different ways of defining effective diabatic states. This illustrates the fact that the definition of effective diabatic states is not unique, thereby the use of a particular definition of diabatic state to interpret chemical reactivity must be justified.

In the CDC-VBSCF method, we use the ratio of the Heitler–London covalent structure and its overlap with the ionic-state **5** in the adiabatic ground state as the criterion to partition the contribution of structure **5** to the respective diabatic states:

$$\frac{(c_5^R)^2}{(c_5^P)^2} = \frac{a_1^2 + a_1 a_5 S_{15}}{a_2^2 + a_2 a_5 S_{25}} \quad (9)$$

where  $S_{15}$  and  $S_{25}$  are the overlap integrals of between VB structures **1** and **5** and between **2** and **5**, respectively. Equation 9 may be interpreted as a partition based on ionic content, defined by

$$Q^R = a_1^2 + a_1 a_5 S_{15} \quad (10a)$$

$$Q^P = a_2^2 + a_2 a_5 S_{25} \quad (10b)$$

Using the condition of eq 9, we obtain the coefficients for structure **5** in the reactant and product effective diabatic states in eqs 3 and 4:

$$c_5^R = N_5 \left( \frac{Q^R}{Q^R + Q^P} \right)^{1/2} a_5 \quad (11)$$

and

$$c_5^P = N_5 \left( \frac{Q^P}{Q^R + Q^P} \right)^{1/2} a_5 \quad (12)$$

where  $N_5$  is a normalizing factor to ensure that  $c_5^R + c_5^P = a_5$ .

A special case may also be considered if we assume the overlap between the ionic (**5**) and covalent VB structure (**1** or **2**) is negligible. Then, we obtain a different set of effective CDC states, which yield the same (exact VBSCF) ground-state wave function:

$$c_5^R = N_5 \left( \frac{a_1^2}{a_1^2 + a_2^2} \right)^{1/2} a_5 \quad (13)$$

$$c_5^P = N_5 \left( \frac{a_2^2}{a_1^2 + a_2^2} \right)^{1/2} a_5 \quad (14)$$

This further emphasizes the “arbitrariness” of defining effective diabatic states, and consequently, conclusions such as quantitative solvent reorganization energies for a chemical reaction derived from such diabatic states.

Having defined these configuration coefficients in the diabatic states, the corresponding matrix elements in eq 6 can be determined accordingly to obtain the ground-state energy. It is clear that the CDC-VB wave function is identical to that of the VBSCF ground state:<sup>37,38</sup>

$$\Phi^{VB} = \Phi^{CDC-VB} = \Phi^R + \Phi^P \quad (15)$$

Consequently, the ground-state energy from the two-state CDC-VB method reproduces the exact energy of VBSCF theory.

**3.2. Variational Diabatic Configuration.** In the variational diabatic configuration VB (VDC-VB) approach, the expectation energy of each effective diabatic state is variationally minimized by optimizing both configuration and orbital coefficients (eqs 3 and 4).<sup>10</sup> Thus, the diagonal Hamiltonian matrix elements are the variational energies of the reactant and product state:

$$\epsilon_{VB}^R = H_{11}^{VDC} = \langle \Phi_{VDC}^R | H | \Phi_{VDC}^R \rangle \quad (16)$$

$$\epsilon_{VB}^P = H_{22}^{VDC} = \langle \Phi_{VDC}^P | H | \Phi_{VDC}^P \rangle \quad (17)$$

where  $\Phi_{VDC}^R$  and  $\Phi_{VDC}^P$  are the VDC diabatic wave functions for the reactant state (eq 3) and the product state (eq 4), respectively. It is important to point out that the energy of the VDC diabatic state always lies below that of the corresponding CDC state by virtue of the variational principle:

$$\epsilon_{VB}^R \leq H_{11}^{CDC} \quad (18)$$

$$\epsilon_{VB}^P \leq H_{22}^{CDC} \quad (19)$$

Clearly, there is distinction between CDC and VDC states in that the former are constructed from the VBSCF states that minimize the adiabatic ground-state energy of the system, whereas the latter are obtained by directly minimizing the energies of the effective diabatic states defined by eqs 3 and 4. The CDC model naturally reproduces the exact VBSCF energy for the ground state because the CDC wave function is identical to that of VBSCF theory by construction (eq 15). On the other hand, the wave function from the two-state VDC model is constructed by linear combination of the two independently optimized effective diabatic states whose orbital coefficients are kept fixed in subsequent VB calculations. Thus, the VDC adiabatic potential energy is higher than that of VBSCF. Alternatively, we can construct a VDC effective Hamiltonian by enforcing the resonance energy  $H_{12}$  in such a way that the lowest energy of the secular determinant for this two-state model is identical to the VBSCF energy.<sup>27,38</sup> However, there is no reason to actually use VDC states to construct an EHVB model to fit the desired adiabatic potential energy because the wave function is not variationally optimized, making the computation of energy gradients extremely difficult.

#### 4. Mixed Molecular Orbital and Valence Bond Theory

We first describe the block-localized wave function (BLW) method for constructing effective diabatic states. Then, we

present the mixed molecular orbital and valence bond (MOVB) theory for optimizing the diabatic-state energies and adiabatic potential energy surface.<sup>4,5,13,14</sup>

**4.1. The Block-Localized Wave Function.** In the mixed molecular orbital and valence bond (MOVB) method,<sup>4,5,13,14</sup> we use Hartree–Fock (HF) theory with localized molecular orbitals to define VB-like resonance states as the basis configurations in VB calculations.<sup>29–36</sup> In this way, each Lewis resonance structure, called diabatic state, is represented by a single Slater determinant wave function, taking advantage of the delocalized nature of molecular orbitals in HF theory. For comparison, in ab initio VB theory, a Lewis resonance structure is typically described by a combination of several covalent and ionic VB structures, e.g., four determinants are needed to specify the reactant state in eq 3. The MOVB wave function for a molecular system is written as a linear combination of these MOVB diabatic states.

$$\Phi_{\text{MOVB}} = \sum_K b_K \Psi_{\text{MOVB}}^K \quad (20)$$

where  $\Psi_{\text{MOVB}}^K$  is the wave function for the  $K$ th MOVB diabatic state, which is defined by using the block-localized wave function (BLW) method.<sup>29–31</sup>

The use of BLW to define strictly localized Lewis resonance structures was introduced by Mo et al.,<sup>29–31</sup> although an earlier application of this localization scheme has been reported for estimation of weak intermolecular interactions and basis set superposition errors.<sup>32–34</sup> The BLW method has been applied to small molecules in the gas phase to rationalize electronic delocalization effects and specific energy components on intermolecular interactions.<sup>30,31,35,36,44–48</sup> It has also been used in MOVB theory, applied to condensed phase systems,<sup>49</sup> including chemical reactions in aqueous solution in combined quantum mechanical and molecular mechanical (QM/MM) simulations.<sup>4,5,13,14</sup>

Specifically, for diabatic-state  $K$ , we partition the system into  $\Omega_K$  subgroups according to the specific Lewis resonance structure. For example, the Lewis structure for the reactant state defined by eq 3 consists of two subgroups (blocks), including  $\text{H}_3\text{N}$  and  $\text{CH}_3\text{NH}_3^+$ , respectively, whereas the pure ionic structure **5** in Scheme 1 is represented by three subgroups:  $\text{H}_3\text{N}$ ,  $\text{CH}_3^+$ , and  $\text{NH}_3$ . The localized wave function for diabatic-state  $K$  is written as a single Slater determinant:

$$\Psi_{\text{MOVB}}^K = \hat{A} \{ \chi_1^K \chi_2^K \dots \chi_{\Omega_K}^K \} \quad (21)$$

where  $\chi_a^K$  is a product of molecular orbitals in the  $a$ th subgroup (block),

$$\chi_a^K = \varphi_{a,1}^K \alpha \varphi_{a,1}^K \beta \dots \varphi_{a,n_a/2}^K \beta \quad (22)$$

where  $\{\varphi_{a,i}^K, i = 1, \dots, n_a/2\}$  are molecular orbitals,  $\alpha$  and  $\beta$  are electronic spin orbitals, and  $n_a$  is the number of electrons in subgroup  $a$ .

We note that molecular orbitals within each block,  $\{\varphi_{a,i}^K, i = 1, \dots, n_a/2\}$ , are orthonormal, whereas orbitals in different blocks are nonorthogonal and have nonzero overlap:

$$\langle \varphi_{a,i}^K | \varphi_{a,j}^K \rangle = \delta_{ab} \quad (23)$$

$$s_{ij}^{ab} = \langle \varphi_{a,i}^K | \varphi_{b,j}^K \rangle \neq 0 \quad a \neq b \quad (24)$$

These features perhaps are best illustrated by the coefficient matrix for the occupied MOs, for diabatic-state  $K$ :

$$\mathbf{C}^K = \begin{pmatrix} \mathbf{C}_1^K & 0 & \dots & 0 \\ 0 & \mathbf{C}_2^K & \dots & 0 \\ \dots & \dots & \dots & \dots \\ 0 & 0 & \dots & \mathbf{C}_{\Omega_K}^K \end{pmatrix} \quad (25)$$

where  $\mathbf{C}_a^K$  is a block matrix of orbital coefficients for orbitals in  $\chi_a^K$  (eq 22).<sup>5</sup>

**4.2. Consistent Diabatic Configuration MOVB (CDC-MOVB).** For the  $\text{S}_{\text{N}}2$  reaction of  $\text{H}_3\text{N}$  and  $\text{CH}_3\text{NH}_3^+$ , we define the reactant and product MOVB diabatic states by the following two Lewis structures:



Note that these two Lewis structures are equivalent to those defined by eqs 3 and 4 in the effective Hamiltonian VB theory; however, four Slater determinants are used in VB theory, whereas a single Slater determinant is employed for each structure in MOVB theory.

The MOVB wave function for the  $\text{S}_{\text{N}}2$  reactive system is a linear combination of the two diabatic states, which is optimized simultaneously with respect to the configuration (eq 20) and orbital (eq 25) coefficients to minimize the MOVB ground-state energy. The individual MOVB diabatic states ( $\Psi_{\text{MOVB}}^{\text{R}}$  and  $\Psi_{\text{MOVB}}^{\text{P}}$ ) are called the CDC states, which can be directly compared with the same type of states (CDC) derived from VBSCF theory.<sup>27,38</sup>

We note that because both the orbital and configuration coefficients are simultaneously optimized, the gradients of the adiabatic potential energy can be conveniently determined in the same fashion as that in conventional multiconfiguration self-consistent field (MCSCF) method or the VBSCF method describe above. The energy derivatives will be reported in a forthcoming paper.

**4.3. Variational Diabatic Configuration MOVB (VDC-MOVB).** The diabatic states of eqs 26a and 26b, which are expressed by eq 21, can be individually variationally optimized, which yield the expectation energies for the reactant and product states ( $\epsilon_{\text{MOVB}}^{\text{R}}$  and  $\epsilon_{\text{MOVB}}^{\text{P}}$ ).<sup>4,5,13,14</sup> These energies are comparable to the corresponding values obtained from the VDC-VB approach introduced above. Similarly, the VDC-MOVB diabatic states can be used to obtain an adiabatic ground-state energy, and such an adiabatic energy can be even optimized to yield the desired barrier height for the  $\text{S}_{\text{N}}2$  reaction by adjusting or scaling the off-diagonal resonance energy,  $H_{12}$ . However, we note that the value of obtaining the VDC diabatic states is not for determining the adiabatic ground-state energy of the system, but rather, the VDC states are useful for investigating the properties of the effective diabatic states.

## 5. Computational Details

All calculations are carried out using the Xiamen Valence bond (XMVB)<sup>27</sup> program modified to include the new features described here and Gaussian03.<sup>50</sup> Geometries for the ammonia exchange  $\text{S}_{\text{N}}2$  reaction along the reaction coordinate defined by eq 5 are optimized at the HF/6-31+G(d,p) level, and the 6-31+G(d,p) basis set is used throughout for all single-point energy calculations, including B3LYP, MP2, CCSD(T) and the three valence bond methods (VBSCF, BOVB and MOVB). In VBSCF and BOVB calculations, the inner electrons are frozen at the Hartree–Fock level and 22 valence electrons are treated

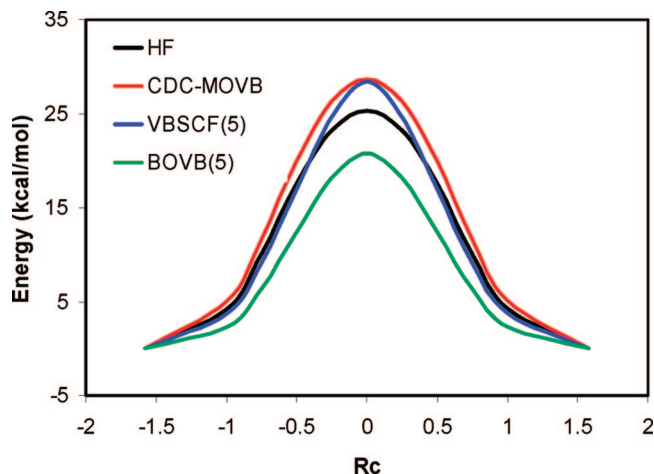


**Figure 3.** Computed adiabatic ground-state potential energy profiles using Hartree–Fock, BOVB, VBSCF, and MOVb methods for the  $S_N2$  reaction between ammonia and the methylammonium ion in the gas phase. The 6-31+G(d,p) basis set is used in all calculations. Relative energies are given in kcal/mol and the reaction coordinate is in angstroms.

**TABLE 1: Computed Binding Energies (kcal/mol) for the Formation of the Ion–Dipole (IP) Complex and the Barrier Heights Relative to the Separate Species (TS) and Relative to the IP Complex ( $\Delta E^\ddagger$ ) for the  $S_N2$  Reaction between  $\text{NH}_3$  and  $\text{CH}_3\text{NH}_3^+$**

	HF	B3LYP	MP2	CCSD(T)	BOVB(5) <sup>a</sup>	VBSCF(5) <sup>a</sup>	MOVb(2) <sup>a</sup>
IP	−8.5	−9.0	−9.5	−9.6	−11.6	−7.8	−8.7
TS	16.8	8.2	14.0	12.3	9.1	20.6	20.0
$\Delta E^\ddagger$	25.3	17.2	23.5	21.9	20.7	28.4	28.7

<sup>a</sup> Value in parentheses is the number of structures used in the calculation.

in VB calculations. Additional specific details are described as the results are presented below.

## 6. Results and Discussion

The main goal of this study is the construction of effective diabatic states and the use of these states to represent the ground-state adiabatic potential energy surface. We first discuss the adiabatic potential energy profile for the ammonia exchange reaction to validate the accuracy of the computational methods used in the present study. Then, we focus on the construction and investigation of the effective diabatic states and the coupling resonance energy to generate the adiabatic potential surface.

**6.1. Adiabatic Potential Energy Surface.** We first consider the adiabatic potential energy profile in Figure 3 for the  $S_N2$  reaction between  $\text{H}_3\text{N}$  and  $\text{CH}_3\text{NH}_3^+$  along the reaction coordinate as defined in eq 5. In this paper, we focus on the region from the ion-dipole (IP) complex in the reactant state to the IP complex of the product for this symmetric exchange reaction. In Table 1, we list the calculated binding energies for the formation of the IP complex between ammonia and methylammonium ion, along with the barrier heights from the IP minimum, from various levels of theory, including HF, B3LYP, MP2, CCSD(T), BOVB(5), VBSCF(5), and MOVb(2), where the number in parentheses are the number configurations used in VB calculations. The 6-31+G(d,p) basis set is used in all computations at the HF/6-31+G(d,p) geometry.

The best results are considered to be from coupled cluster calculations at the CCSD(T) level. Thus, both HF and MP2 slightly overestimate the energy barrier from the IP complex state in comparison with the coupled cluster data, whereas

density functional theory using B3LYP underestimates the barrier height by about 5 kcal/mol. In all, the breathing orbital valence bond (BOVB) theory with 5 or 6 (see Figure 2) configurations performs exceptionally well for the present  $S_N2$  reaction in comparison with CCSD(T) results with a computed barrier within 1 and 2 kcal/mol, respectively. The VBSCF(5) computations yield an energy barrier about 3 kcal/mol greater than that from HF theory (25.3 kcal/mol), whereas the two-state CDC-MOVb method produced a nearly identical energy of activation (28.7 kcal/mol) as that from VBSCF. Importantly, Figure 3 demonstrates that the CDC-MOVb approach can yield adequate ground-state adiabatic potential energy surface for a chemical reaction as illustrated by the present  $S_N2$  process. Overall, the VBSCF and CDC-MOVb results are comparable. Because these two methods are qualitatively similar, which include partial static correlations, they are used for comparison and discussion presented below. The BOVB theory also include some dynamic correction effects, which represents a higher level of theory than MOVb.

**6.2. Diabatic States.** The second goal of this study is to derive effective diabatic states from the ground-state adiabatic potential energy surface to describe the change in electronic structure for the “reactant” and “product” states along the reaction coordinate. These effective diabatic states can, in turn, be used to construct the adiabatic potential energy surface,<sup>2,4,5,8,18–20,51,52</sup> and to determine properties of the reacting system, including the reaction coordinate as defined in Marcus theory of electron transfer and the calculation of solvent reorganization energy for condensed phase reactions.<sup>14</sup> As already noted above, unfortunately, there is no unique way of defining such effective diabatic states because molecular wave functions have nonzero and non-negligible overlap between the reacting fragments. Therefore, one has to rely on some physically meaningful approximations to construct such effective diabatic states for qualitative analysis and for quantitative investigation of chemical reactivity, and the latter needs to be validated by comparison with relevant experimental data and consistent theories.<sup>14</sup> The present paper is concerned with the intrinsic potential energy surface and diabatic states in the gas phase, whereas studies of solvent effects shall be addressed in another paper.

Nevertheless, the term, reactant state or product state, does have a well-defined meaning when the reacting partners are fully separated, which can be fully characterized by the corresponding Lewis resonance structures.<sup>2</sup> This consideration provides a physical approach for defining the effective diabatic states, given in eqs 3 and 4, to represent the fundamental features of chemical bonding and charge polarization of the reactant state and product state, respectively. Using eqs 3 and 4 as the definition of the effective diabatic states, the partition of the ionic VB configuration(s) into the individual diabatic states leads to two computational approaches, and the results have different physical interpretations of effective diabatic states.

In the first approach, the adiabatic ground-state energy is variationally minimized by optimizing both the orbital and configuration coefficients, and the resulting effective diabatic states are called consistent diabatic configurations (CDC), which are depicted in Figure 4. Using ab initio VBSCF configurations, we can construct the CDC states based on the ratio of ionic content, resulting from the overlap between the ionic configuration (5) and the corresponding reactant (1) or product covalent (2) structure (see eqs 11 and 12). Thus, the CDC-VBSCF states are obtained by mixing three VB structures, consisting of four determinant wave functions for the present  $S_N2$  reaction.



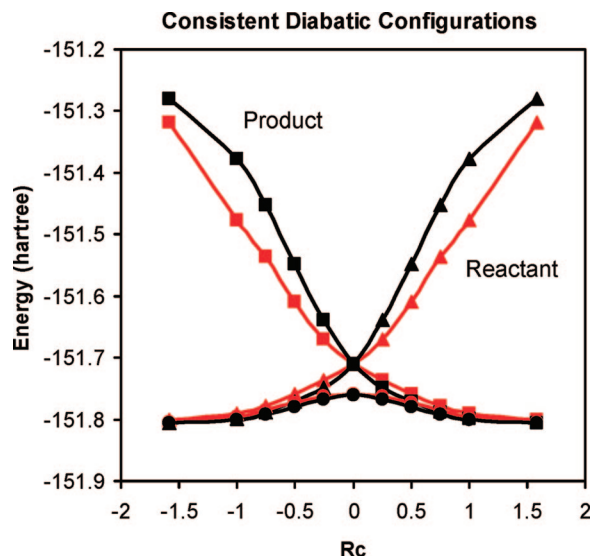


**Figure 4.** Consistent diabatic configurations for the reactant and product states for the  $S_N2$  reaction between ammonia and the methylammonium ion from ab initio VB theory (black) and from the mixed MOVB theory (red). The variational adiabatic ground-state energy profiles are also shown. Total energies are given in atomic units (hartrees) and the reaction coordinate in angstroms.

Alternatively, if we use Hartree–Fock theory with block-localized molecular orbitals, which is represented by a single Slater determinant, to approximate the same Lewis structures, the variational minimization of the adiabatic ground-state energy yields the CDC-MOVB diabatic states.

Both the CDC-MOVB and CDC-VBSCF states are obtained on the basis of minimization of the adiabatic ground-state energy, and thus, they are fully comparable, keeping in mind that MOVB is much more efficient computationally than ab initio VB calculations. Figure 4 shows that the CDC diabatic states from ab initio VBSCF and from ab initio MOVB theories are in remarkable agreement, especially in view of the fact that a total of five VB structures, represented by seven determinants, are used in the former approach, whereas only two determinants are needed in MOVB, one for each diabatic state. At the corresponding minimum geometry (IP complex) of a given diabatic state, the total electronic energy from VBSCF theory is lower than that obtained using MOVB by 2.8 kcal/mol for the ammonia exchange reaction. If we focus on the reactant state, the energy of the CDC state increases sharply, varying as much as 0.525 hartree (330 kcal/mol) in both VBSCF and MOVB calculations, as the molecular geometry changes from the reactant IP complex to the product IP complex. Furthermore, it is interesting to note that the CDC-MOVB energy becomes lower than the CDC-VBSCF value beyond the transition state at  $R_c = 0$  Å, as the molecular geometry significantly deviates from the minimum of the diabatic state. This suggests that the MOVB electronic configuration contains somewhat more ionic character than that in the CDC-VBSCF state.<sup>9,10</sup> Recall that the ionic configuration (5) has a lower energy than the covalent state (1) beyond  $R_c = -0.5$  Å, midway between the IP complex and transition state (Figure 1).

In the second approach, which is called the variational diabatic configuration (VDC) model, the effective diabatic states defined by eqs 3 and 4 in VBSCF theory,<sup>27,37,38</sup> and those by eqs 21 and 26 in MOVB theory, are independently variationally minimized to obtain the best diabatic-state energy for each individually state,<sup>4,5</sup> irrespective to the adiabatic ground-state energy. Therefore, unlike the CDC model, there is no relation-

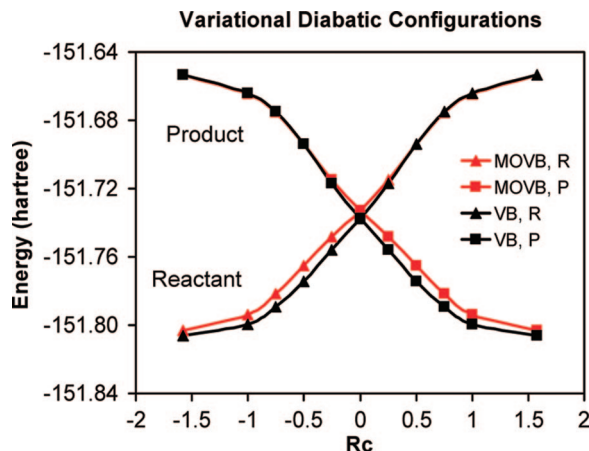


**Figure 5.** Variational diabatic configurations for the reactant and product states for the  $S_N2$  reaction between ammonia and the methylammonium ion from ab initio VB theory (black) and from the mixed MOVB theory (red). Total energies are given in atomic units (hartrees) and the reaction coordinate in angstroms.

ship between configuration and orbital coefficients in eqs 3 and 4 and those from full VBSCF calculations. The molecular wave function using VDC states does not yield the same adiabatic ground-state energy and its value is necessarily greater than that from the CDC method. However, it is important to note that the VDC states give the minimum energies of the effective diabatic states. Thus, a distinction is made such that the diagonal terms in the CDC model are simply elements of the Hamiltonian,  $H_{11}^{CDC}$  and  $H_{22}^{CDC}$ , whereas those in the VDC model are true variational energies of the reactant and product states:  $\epsilon^R = H_{11}^{VDC}$ , and  $\epsilon^P = H_{22}^{VDC}$ .

The computed energies of the VDC reactant and product states using VBSCF and MOVB are compared in Figure 5. The most striking feature is that the agreement between these two computational approaches is exceedingly good, particularly for energies greater than the crossing point at the transition state. This is in contrast to the CDC model in that the region that has greater deviations between VBSCF and MOVB results is in the high energy states (Figure 4). Clearly, the variational optimization of both covalent and ionic configurations in the diabatic states in the VBSCF approach enhances the contributions of ionic character, which significantly lowers the total diabatic-state energy. Of course, the delocalized nature of molecular orbitals (within each block of molecular fragment) in MOVB can reasonably describe the relative contributions of ionic structures when they are dominant.

Aside from these qualitative differences between CDC and VDC states, there are also two major quantitative differences. First, we note that the energy variation in the VDC states is more modest than the corresponding change in the CDC state in going from the reactant to the product state, and vice versa. The total energy increase for the reactant state is 0.153 hartree (95 kcal/mol) in the VDC model, which is less than one-third of the change of 0.525 hartree (330 kcal/mol) from CDC calculations. This is not surprising in view of the fact that the ionic configuration has much lower energy than the covalent configuration for the reactant state in the product geometry (Figure 1). This is also reflected by the configuration weight for the ionic structure determined by the CDC and VDC method (Figure 6).<sup>53</sup> Second, the reactant and product diabatic states cross at about the same point, within 0.005 hartree (3 kcal/mol), from the VBSCF and MOVB calculations either in the CDC or in the VDC model. However, the energies of crossing,  $\Delta E_c$ ,

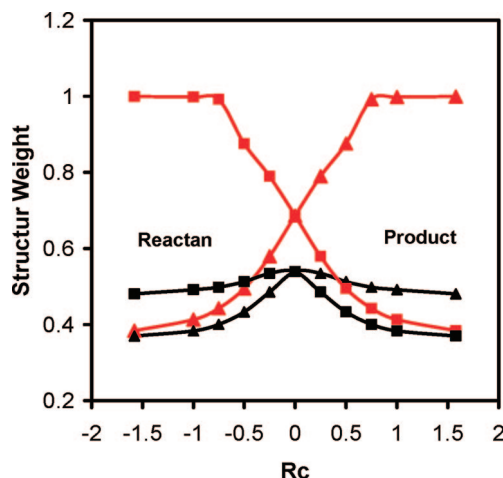


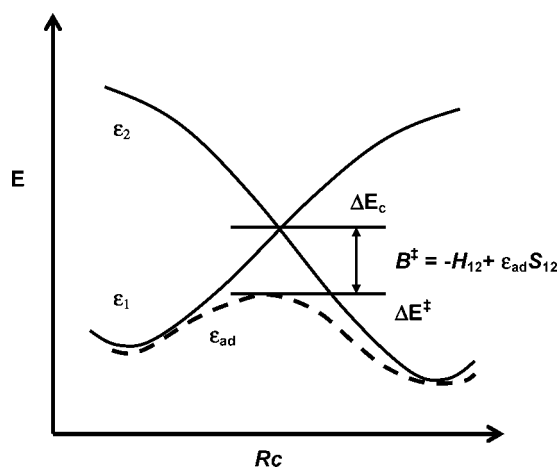
**Figure 6.** Configuration weight for the ionic configuration 5 in the reactant and product effective diabatic states defined by the CDC (black) and VDC (red) model using VBSCF theory. The weights of VB structures are determined by use of Coulson–Chirgwin formula  $w_K = \sum_L a_K a_L \langle \Psi_K | \Psi_L \rangle$ , see ref 53. The reaction coordinate is given in angstroms.

determined by the CDC and the VDC method are very different. The crossing energy from CDC-VBSCF is 60 kcal/mol (0.095 hartree), whereas the value from VDC-VBSCF is 43 kcal/mol (0.069 hartree). The difference between the two models is nearly as large as the entire barrier height for the chemical reaction (Table 1).

We also note that the good agreement between VBSCF and MOVb theories on the computed effective diabatic states, both using the CDC and VDC models, shows that the computationally efficient MOVb method is a reliable technique for constructing diabatic-state and adiabatic-state potential energy surfaces. We further remark that even though MOVb utilizes delocalized molecular orbitals within each block-localized fragment, it is capable of modeling the CDC states derived from VBSCF, which is primarily covalent in nature (it is almost 50%–50% mixture according to Figure 6). The remarkable coupling of these configurations to yield the adiabatic ground-state energy, which is described next, apparently ensures the CDC states converge to the correct ones that minimize the ground-state energy of the system. Ab initio valence bond theory represents the most reliable electronic structural method for studying chemical reactions, in addition to its unique advantage of providing intuitive chemical insights. VBSCF calculations include static electron correlations, comparable to CASSCF.<sup>40</sup> In a forthcoming study, we compare the performance of MOVb with BOVB theories by an effective Hamiltonian approach; the latter also incorporates dynamic electron correlation effects.

In closing, we further emphasize the fact that there are two fundamentally different ways of constructing effective diabatic states; in fact, there are infinite number of ways doing so between these two limiting cases. In the CDC method, the *diabatic* states are derived from the VB configurations that minimize the adiabatic ground-state energy, which is the primary quantity of interest. By comparing Figures 1 and 4, it is clear that the CDC states stay roughly on the potential energy surface of the covalent configuration, decorated by some mixture of the ionic structure (5). Of course, this mixing is not optimal as far as the diabatic-state energy is concerned. On the other hand, it is the diabatic-state energy that is minimized in the VDC approach, which converges from a dominantly covalent configuration at the geometry of energy minimum in that state to

## SCHEME 2: Illustration of Diabatic and Adiabatic Potential Energy Surfaces, and the Energy of Crossing, the Activation Barrier and the Resonance Energy at the Transition State



an ionic configuration at the highly distorted geometry corresponding to the minimum of the opposite state. Therefore, it may be interpreted that CDC and VDC states represent different electronic configurations in going from the reactant to the product geometry, although both models start off in the same electronic configuration at the respective minimum.

The fundamental difference between CDC and VDC diabatic states has important implications in the study of condensed phase reactions.<sup>14</sup> An immediate question is which diabatic state should be employed, CDC or VDC, to define the Marcus energy gap reaction coordinate and to determine the associated solvent reorganization energy. These issues are beyond the scope of this paper and will be presented in another forthcoming study in which we carry out molecular dynamics simulations using combined quantum mechanical and molecular mechanical (QM/MM) potentials.<sup>54–56</sup> In these studies, various combinations of the CDC-MOVb and VDC-MOVb approaches as the QM model are examined.

**6.3. Resonance Energy.** The definition and construction of effective diabatic states provides a starting point for building the adiabatic potential energy surface of the ground state. An equally important factor is the electronic coupling, or resonance energy, between the effective diabatic states. In the VB correlation diagram for a chemical reaction introduced by Shaik,<sup>2</sup> the resonance energy,  $B$ , is the stabilization energy of the diabatic states at the crossing point ( $\Delta E_c$ ) to yield the adiabatic transition state of the chemical reaction (Scheme 2). Thus,

$$B = \Delta E_c - \Delta E^\ddagger \quad (27)$$

where  $\Delta E^\ddagger$  is the adiabatic ground-state energy of activation. A number of approximate and empirical expressions have been used to estimate the resonance energy and to correlate with chemical reactivity, including linear free energy relationships widely used in physical organic chemistry.  $B$  can also be related to the singlet–triplet energy gap,  $\Delta E_{ST}^\pm$ , at the transition state in a two-state model by<sup>2,57</sup>

$$B^\ddagger = \frac{1}{2}(1 - S_{12}^\ddagger)\Delta E_{ST}^\ddagger \quad (28)$$

where  $S_{12}$  is the overlap integral between the reactant and product states at the crossing point.



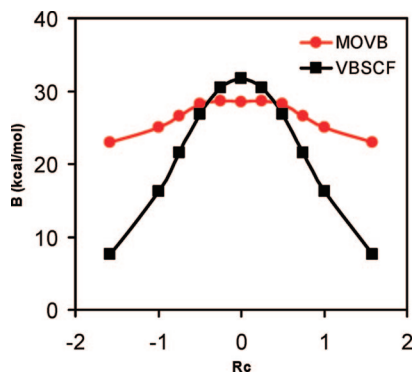


**Figure 7.** Computed resonance energy (kcal/mol) along the reaction coordinate (in angstroms) for the  $S_N2$  reaction between ammonia and the methylammonium ion using the CDC-MOVB (red) and CDC-VBSCF (black) method.

Considering the secular equation in eq 6, one readily obtains an expression for the resonance energy along the reaction coordinate as follows:

$$B(R_c) = -[H_{12}(R_c) - \epsilon_{ad}(R_c)S_{12}(R_c)] \quad (29)$$

where  $R_c$  is the reaction coordinate,  $\epsilon_{ad}$  is the adiabatic ground-state energy, and  $H_{12} = \langle \Phi^R | H | \Phi^P \rangle$  is the exchange integral between the reactant and product diabatic states. Because all quantities on the right-hand side of eq 29 are known in our CDC model, in both ab initio VBSCF and ab initio MOVB methods, the resonance energy can be directly computed and the results along the reaction coordinate are shown in Figure 7. Apparently, the variation of the resonance energy from CDC-VBSCF calculations is different than that from the CDC-MOVB method. In the former approach,  $B(R_c)$  shows a greater dependence on the reaction coordinate than that of the CDC-MOVB model, whereas the latter shows a rather flat variation. In CDC-VBSCF, the largest resonance stabilization (31.7 kcal/mol) occurs at the transition state,  $B^\ddagger$ , where the interacting (reactant and product) states have the same energy ( $E_c$ ). The resonance energy at the IP complex,  $B(R_{IP})$ , is much smaller (7.6 kcal/mol). For comparison, the corresponding CDC-MOVB values are 28.6 kcal/mol for  $B^\ddagger$  and 22.9 kcal/mol for  $B(R_{IP})$ ; the  $B$  value at the transition state is in fact a small minimum of 0.1 kcal/mol in this case. The relatively large  $B$  value, away from the transition state, in CDC-MOVB calculations is a reflection of greater ionic character in the MOVB diabatic state than in the CDC-VBSCF estimate. Despite the differences in individual diabatic state and in resonance energy, the overall adiabatic ground-state energy curves are still in reasonable agreement between MOVB and VBSCF (Figure 2).

Obviously, there is difference between resonance energy  $B$  and exchange integral  $H_{12}$  (eq 29); these two quantities are only identical if the overlap integral between the reactant and product states is zero. The significance of the overlap integral is also clear in view of singlet–triplet energy gap (eq 28). In Figure 8, we illustrate the computed overlap integral  $S_{12}$  from CDC-MOVB and CDC-VBSCF calculations. Clearly, the trends of the resonance energy mirror nicely the variation in the overlap (see Figures 7 and 8). This is not surprising because the exchange integral also depends on the overlap of the two interacting states. Moreover, Figure 8 shows that the overlap integral between the two diabatic states, either from VBSCF or from MOVB calculations, is anything but negligible, an essence of valence bond theory and a matter of inconvenience in molecular systems. However, in empirical treatments of valence bond states in which orbitals are implicit,<sup>58</sup> the overlap integral

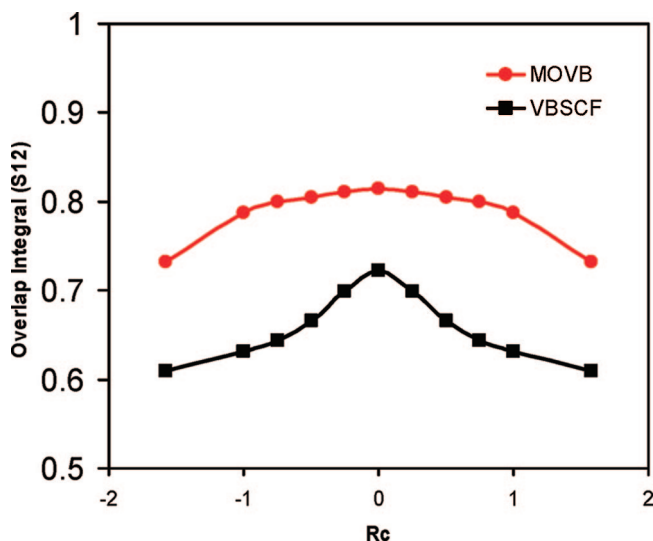


**Figure 8.** Computed overlap integral between the reactant and product diabatic states along the reaction coordinate for the  $S_N2$  reaction between ammonia and the methylammonium ion using the CDC-MOVB (red) and CDC-VBSCF (black) method. The reaction coordinate is given in angstroms.

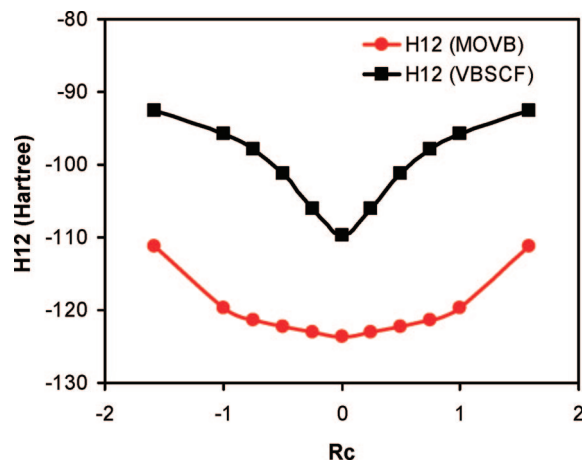


**Figure 9.** Computed exchange integral,  $H_{12}$ , between the reactant and product diabatic states along the reaction coordinate for the  $S_N2$  reaction between ammonia and the methylammonium ion using the CDC-MOVB (red) and CDC-VBSCF (black) method. The reaction coordinate is given in angstroms.

is generally assumed to be zero. In this case, the resonance energy  $B$  ought to be fitted to reproduce accurate results as a function of molecular geometry as done, for example, in the exceptionally successful MMVB (molecular mechanics with valence bond) approach developed by Robb and co-workers.<sup>59</sup> Although  $B$  can be fitted to reproduce the energy of a single point (e.g., the barrier  $\Delta E^\ddagger$  for a given reaction),<sup>58</sup> it is not guaranteed that the entire potential energy surface can be adequately described by such empirical models.<sup>4,5,7,8,19,20</sup>

In general,  $B$  depends on both the exchange integral and the total adiabatic ground-state energy itself (see also eq 29). The striking difference in these quantities is apparent by comparing the total energy of the exchange integral in Figure 9 with that of the resonance energy in Figure 7, keeping in mind that the total energy of the adiabatic ground-state energy is in the order of  $-151.8$  hartree. Although the coupling resonance energy of 37 kcal/mol is considered very large,<sup>60</sup> the absolute energies of the exchange integral and adiabatic ground-state dwarf that of the resonance energy. Overall, the MOVB method yields

greater exchange and overlap integrals than the corresponding CDC-MOVb results because block-localized molecular orbitals used in MOVb contain more significant ionic characters, resulting in greater overlap between the two effective states. Finally, we comment that eq 29 provides a practical approach for investigating the effects of solvation on the resonance energy  $B$  through combined QM/MM simulations.

## 7. Conclusions

Previously, we developed a mixed molecular orbital and valence bond (MOVb) theory for the construction of diabatic-state and adiabatic potential energy surfaces for modeling chemical reactions in solution.<sup>4,5</sup> In this approach, the valence bond-like structures that define the effective diabatic states for the reactant and product configurations, as well as any other relevant Lewis resonance structures, are represented by a block-localized wave function (BLW) method.<sup>29–31</sup> The energy of each diabatic state is variationally minimized, and then used as the basis function to build the adiabatic potential energy surface along the reaction coordinate. This corresponds to the present VDC-MOVb method. Using these effective diabatic states, we have studied a number of chemical reactions in solution, including a series of nucleophilic substitution reactions of all four types,<sup>4,14</sup> and proton-transfer reactions.<sup>5,13</sup> The development of this ab initio MOVb approach allows for a definition of the solvent reaction coordinate, in terms of Marcus theory energy gap for electron-transfer reactions,<sup>61</sup> on the basis of first principles, and the computation of solvent reorganization energy and the diabatic-state coupling along the reaction coordinate.<sup>14</sup>

In this work, we present a theoretical model for deriving the effective diabatic states from ab initio self-consistent field valence bond (VBSCF) theory by systematically reducing the multiconfigurational VB Hamiltonian into an effective two-state model, making use of a nucleophilic substitution reaction as an illustrating example. We first introduce a general principle for defining effective diabatic states, on the basis of Lewis resonance structures of the fully separated reactant partners, or product partners (of course, this approach is a standard application of valence bond theory). Then, we describe two computational models for the optimization of the effective diabatic states, resulting in two ways of interpreting such effective diabatic states. This is the most significant result of this paper. The first model is called the variational diabatic configuration (VDC) method, in which the energies of the individual diabatic states are variationally minimized. The VDC model is identical to the original computational method used in the MOVb theory,<sup>5</sup> although we have generalized it to ab initio valence bond theory in the present study. The VDC states can then be used as basis functions, without further optimization, in valence bond calculations,<sup>4,5</sup> and in principle, an effective Hamiltonian can be constructed by enforcing the resonance energy to reproduce the exact VBSCF surface or experimental data. In the second model, which is termed as the consistent diabatic configuration (CDC) method, both the configuration coefficients and orbital coefficients are simultaneously optimized to minimize the adiabatic ground-state energy in VBSCF or in MOVb calculations. Obviously, the VB wave function obtained from CDC states minimizes the adiabatic ground-state energy of the system.

We make use of the symmetric  $S_N2$  reaction between  $H_3N + CH_3NH_3^+$  to construct the CDC and VDC diabatic and adiabatic potential surfaces at the VBSCF and the MOVb levels of theory, employing the 6-31+G(d,p) basis set. The ab initio VB results are used to validate the MOVb method, which is much more efficient computationally. Overall, the MOVb results

are in excellent agreement with VBSCF calculations, both in the computed diabatic and in the adiabatic potential energy surfaces, suggesting that MOVb can be used as an efficient alternative to ab initio VB theory for modeling chemical reactions in solution and in enzymes.

On the basis of the computational results, we make the following two observations.

(1) The CDC and VDC states converge to different valence bond configurations along the reaction coordinate, which show markedly different energy variations. The CDC diabatic states vary as much as 330 kcal/mol in energy as the molecular geometry varies between the two ion–dipole complex regions, whereas the energies of the VDC diabatic states change about 95 kcal/mol along the reaction coordinate. The VDC state is represented by a dominantly covalent configuration (**1** or **2**) at the respective minimum geometry of the ion-dipole complexes, and changes to a state best described by the ionic configuration (**5**) along the reaction path. On the other hand, the CDC state stays mainly on the corresponding covalent state mixed with the high-energy ionic states. The qualitative and quantitative differences between the CDC and VDC diabatic states have important implications in condensed phase reactions, including the estimation of solvent reorganization energy, a subject of subsequent investigations.

(2) The resonance energy, which lowers the energy of crossing between the two effective diabatic states to yield the adiabatic transition state of the reaction, and its variation along the reaction coordinate has a strong dependence on the overlap integral of the two diabatic states. The electronic coupling or resonance energy is estimated to be about 40–60 kcal/mol, as a result of the energy difference between the exchange integral and the ground-state energy scaled by the overlap integral. Although the resonance energy is not affected by the absolute values of the electronic energy of the diabatic and adiabatic states (i.e., the definition of zero energy of the system), the distinction between the exchange integral ( $H_{12}$ ) and the resonance energy ( $B$ ) is clearly reflected and emphasized by their markedly different values (Figures 7 and 9) as a result of *overlap* between diabatic states.

The resonance energy  $B$  is an explicit function of the overlap integral  $S_{12}$ ; however, in empirical models based on VB theory, the resonance energy is typically written as an *implicit* function of  $S_{12}$ , fitted to reproduce the adiabatic potential energy surface. Consequently, molecular fragments or stable compounds can be used as models to fit the potential surface of the effective diabatic states. Recent methods (it is not the aim of this article to discuss the early uses of empirical VB in chemical dynamics calculations and other applications) belonging to this category include molecular mechanics with valence bond (MMVB),<sup>59</sup> multiconfigurational molecular mechanics (MCM),<sup>7,8</sup> multistate empirical valence bond (MS-EVB),<sup>15</sup> and the generalized Gaussian algorithm of Schlegel and Sonnenberg<sup>19,20</sup> and Chang and Miller.<sup>12</sup> Of course, our ab initio MOVb method treats all terms explicitly and the exchange integral can be scaled to construct an MOVb effective Hamiltonian. These empirical VB models, which should not be confused with the EVB model of ref 58 despite an identical acronym, generate the proper potential energy surface, capable of producing the correct transition-state structure and vibrational frequencies,<sup>12,19,20</sup> which can be used to compute a variety of properties, including kinetic isotope effects. An alternative view is that the effective diabatic states are orthogonalized, because the overlap certainly cannot be neglected (Figure 8), such that the resonance energy is the exchange integral itself and independent of the overlap,<sup>62</sup> thereby

overcoming the crucial “overlap problem”. However, in this representation, molecular fragments and real molecules cannot be used as model systems to parametrize such orthogonal diabatic states because the wave functions of independent, real molecules are not orthogonal. Models based on this view employ a simple function term,<sup>58</sup> often a constant value, to represent  $B$  (i.e.,  $H_{12}$  here), fitted to reproduce the desired reaction barrier without considering the detailed adiabatic potential surface. Consequently, this type of empirical valence bond (EVB)<sup>58</sup> “is not flexible enough to fit frequencies at the transition state”,<sup>19</sup> and thus, not suited for computing kinetic isotope effects. Moreover, the resonance energy is assumed to be identical in the gas phase and in solution as well as in the enzyme.<sup>15,18,63</sup> However, unless there is a fortuitous cancelation of energy terms between the valence bond exchange integral  $H_{12}$  and the adiabatic ground-state energy  $\epsilon_{\text{ad}}$  (scaled by the overlap integral) along the entire reaction coordinate, the resonance energy is expected to be dependent on solvation. The theory presented in this work provides a rigorous formulation to address these questions in future studies.

**Acknowledgment.** We thank the National Institutes of Health (GM46736) and the Office of Naval Research for support of this work.

## References and Notes

- (1) Shaik, S. S. *J. Am. Chem. Soc.* **1981**, *103*, 3692.
- (2) Shaik, S.; Shurki, A. *Angew. Chem., Int. Ed.* **1999**, *38*, 587.
- (3) Hiberty, P. C.; Shaik, S. *J. Comput. Chem.* **2007**, *28*, 137.
- (4) Mo, Y.; Gao, J. *J. Comput. Chem.* **2000**, *21*, 1458.
- (5) Mo, Y.; Gao, J. *J. Phys. Chem. A* **2000**, *104*, 3012.
- (6) Mo, Y. *J. Chem. Phys.* **2007**, *126*, 224104/1.
- (7) Kim, Y.; Corchado, J. C.; Villa, J.; Xing, J.; Truhlar, D. G. *J. Chem. Phys.* **2000**, *112*, 2718.
- (8) Tishchenko, O.; Truhlar, D. G. *J. Phys. Chem. A* **2006**, *110*, 13530.
- (9) Su, P.; Ying, F.; Wu, W.; Hiberty, P. C.; Shaik, S. *ChemPhysChem* **2007**, *8*, 2603.
- (10) Song, L.; Wu, W.; Hiberty, P. C.; Shaik, S. *Chem.-Eur. J.* **2006**, *12*, 7458.
- (11) Sini, G.; Shaik, S.; Hiberty, P. C. *J. Chem. Soc., Perkin Trans. 2* **1992**, 1019.
- (12) Chang, Y. T.; Miller, W. H. *J. Phys. Chem.* **1990**, *94*, 5884.
- (13) Gao, J.; Mo, Y. *Prog. Theor. Chem. Phys.* **2000**, *5*, 247.
- (14) Gao, J.; Garcia-Viloca, M.; Poulsen, T. D.; Mo, Y. *Adv. Phys. Org. Chem.* **2003**, *38*, 161.
- (15) Minichino, C.; Voth, G. A. *J. Phys. Chem. B* **1997**, *101*, 4544.
- (16) Wang, F.; Voth, G. A. *J. Chem. Phys.* **2005**, *122*, 144105–1.
- (17) Gwaltney, S. R.; Rosokha, S. V.; Head-Gordon, M.; Kochi, J. K. *J. Am. Chem. Soc.* **2003**, *125*, 3273.
- (18) Hong, G.; Rosta, E.; Warshel, A. *J. Phys. Chem. B* **2006**, *110*, 19570.
- (19) Schlegel, H. B.; Sonnenberg, J. L. *J. Chem. Theory Comput.* **2006**, *2*, 905.
- (20) Sonnenberg, J. L.; Schlegel, H. B. *Mol. Phys.* **2007**, *105*, 2719.
- (21) Song, L.; Wu, W.; Zhang, Q.; Shaik, S. *J. Phys. Chem. A* **2004**, *108*, 6017.
- (22) Song, L.; Wu, W.; Dong, K.; Hiberty, P. C.; Shaik, S. *J. Phys. Chem. A* **2002**, *106*, 11361.
- (23) Cooper, D. L.; Gerratt, J.; Raimondi, M. *Adv. Chem. Phys.* **1987**, *69*, 319.
- (24) Goddard, W. A., III; Dunning, T. H., Jr.; Hunt, W. J.; Hay, P. J. *Acc. Chem. Res.* **1973**, *6*, 368.
- (25) McWeeny, R. *Pure Appl. Chem.* **1989**, *61*, 2087.
- (26) Hiberty, P. C.; Flament, J. P.; Noizet, E. *Chem. Phys. Lett.* **1992**, *189*, 259.
- (27) Song, L.; Mo, Y.; Zhang, Q.; Wu, W. *J. Comput. Chem.* **2005**, *26*, 514.
- (28) Wu, W.; Song, L.; Cao, Z.; Zhang, Q.; Shaik, S. *J. Phys. Chem. A* **2002**, *106*, 2721.
- (29) Mo, Y.; Peyerimhoff, S. D. *J. Chem. Phys.* **1998**, *109*, 1687.
- (30) Mo, Y.; Zhang, Y.; Gao, J. *J. Am. Chem. Soc.* **1999**, *121*, 5737.
- (31) Mo, Y.; Gao, J.; Peyerimhoff, S. D. *J. Chem. Phys.* **2000**, *112*, 5530.
- (32) Gianinetti, E.; Raimondi, M.; Tornaghi, E. *Int. J. Quantum Chem.* **1996**, *60*, 157.
- (33) Gianinetti, E.; Vandoni, I.; Famulari, A.; Raimondi, M. *Adv. Quantum Chem.* **1998**, *31*, 251.
- (34) Raimondi, M.; Famulari, A.; Specchio, R.; Sironi, M.; Moroni, F.; Gianinetti, E. *THEOCHEM* **2001**, *573*, 25.
- (35) Khaliullin, R. Z.; Head-Gordon, M.; Bell, A. T. *J. Chem. Phys.* **2006**, *124*, 204105–1.
- (36) Khaliullin, R. Z.; Cobar, E. A.; Lochan, R. C.; Bell, A. T.; Head-Gordon, M. *J. Phys. Chem. A* **2007**, *111*, 8753.
- (37) Van Lenthe, J. H.; Verbeek, J.; Pulay, P. *Mol. Phys.* **1991**, *73*, 1159.
- (38) van Lenthe, J. H.; Dijkstra, F.; Havenith, R. W. A. *Theor. Comput. Chem.* **2002**, *10*, 79.
- (39) Mo, Y.; Lin, Z.; Wu, W.; Zhang, Q. *J. Phys. Chem.* **1996**, *100*, 11569.
- (40) Thorsteinsson, T.; Cooper, D. L.; Gerratt, J.; Karadakov, P. B.; Raimondi, M. *Theor. Chim. Acta* **1996**, *93*, 343.
- (41) Hiberty, P. C.; Humbel, S.; Archirel, P. *J. Phys. Chem.* **1994**, *98*, 11697.
- (42) Heitler, W.; London, F. Z. *Phys.* **1927**, *44*, 455.
- (43) Martin, C. H.; Graham, R. L.; Freed, K. F. *J. Phys. Chem.* **1994**, *98*, 3467.
- (44) Mo, Y.; Gao, J. *J. Phys. Chem. A* **2001**, *105*, 6530.
- (45) Mo, Y.; Subramanian, G.; Gao, J.; Ferguson, D. M. *J. Am. Chem. Soc.* **2002**, *124*, 4832.
- (46) Mo, Y.; Wu, W.; Song, L.; Lin, M.; Zhang, Q.; Gao, J. *Angew. Chem., Int. Ed.* **2004**, *43*, 1986.
- (47) Mo, Y.; Gao, J. *Acc. Chem. Res.* **2007**, *40*, 113.
- (48) Brauer, C. S.; Craddock, M. B.; Kilian, J.; Grumstrup, E. M.; Orilall, M. C.; Mo, Y.; Gao, J.; Leopold, K. R. *J. Phys. Chem. A* **2006**, *110*, 10025.
- (49) Mo, Y.; Gao, J. *J. Phys. Chem. B* **2006**, *110*, 2976.
- (50) Frisch, M. J.; Trucks, G. W.; Schlegel, H. B.; Scuseria, G. E.; Robb, M. A.; Cheeseman, J. R.; Montgomery, J. A., Jr.; Vreven, T.; Kudin, K. N.; Burant, J. C.; Millam, J. M.; Iyengar, S. S.; Tomasi, J.; Barone, V.; Mennucci, B.; Cossi, M.; Scalmani, G.; Rega, N.; Petersson, G. A.; Nakatsuji, H.; Hada, M.; Ehara, M.; Toyota, K.; Fukuda, R.; Hasegawa, J.; Ishida, M.; Nakajima, T.; Honda, Y.; Kitao, O.; Nakai, H.; Klene, M.; Li, X.; Knox, J. E.; Hratchian, H. P.; Cross, J. B.; Bakken, V.; Adamo, C.; Jaramillo, J.; Gomperts, R.; Stratmann, R. E.; Yazyev, O.; Austin, A. J.; Cammi, R.; Pomelli, C.; Ochterski, J. W.; Ayala, P. Y.; Morokuma, K.; Voth, G. A.; Salvador, P.; Dannenberg, J. J.; Zakrzewski, V. G.; Dapprich, S.; Daniels, A. D.; Strain, M. C.; Farkas, O.; Malick, D. K.; Rabuck, A. D.; Raghavachari, K.; Foresman, J. B.; Ortiz, J. V.; Cui, Q.; Baboul, A. G.; Clifford, S.; Cioslowski, J.; Stefanov, B. B.; Liu, G.; Liashenko, A.; Piskorz, P.; Komaromi, I.; Martin, R. L.; Fox, D. J.; Keith, T.; Al-Laham, M. A.; Peng, C. Y.; Nanayakkara, A.; Challacombe, M.; Gill, P. M. W.; Johnson, B.; Chen, W.; Wong, M. W.; Gonzalez, C.; Pople, J. A. *Gaussian03*; Gaussian, Inc.: Wallingford, CT, 2004.
- (51) Lin, H.; Zhao, Y.; Tishchenko, O.; Truhlar, D. G. *J. Chem. Theory Comput.* **2006**, *2*, 1237.
- (52) Day, T. J. F.; Soudackov, A. V.; Cuma, M.; Schmitt, U. W.; Voth, G. A. *J. Chem. Phys.* **2002**, *117*, 5839.
- (53) Chirgwin, H. B.; Coulson, C. A. *Proc. R. Soc. London, Ser. A* **1950**, *2*, 196.
- (54) Gao, J. *J. Phys. Chem.* **1992**, *96*, 537.
- (55) Gao, J. Methods and applications of combined quantum mechanical and molecular mechanical potentials. In *Reviews in Computational Chemistry*; Lipkowitz, K. B., Boyd, D. B., Eds.; VCH: New York, 1995; Vol. 7, pp 119.
- (56) Gao, J. *J. Comput. Chem.* **1997**, *18*, 1062.
- (57) Shaik, S.; Reddy, A. C. *J. Chem. Soc., Faraday Trans.* **1994**, *90*, 1631.
- (58) Warshel, A.; Weiss, R. M. *J. Am. Chem. Soc.* **1980**, *102*, 6218.
- (59) Bernardi, F.; Olivucci, M.; Robb, M. A. *J. Am. Chem. Soc.* **1992**, *114*, 1606.
- (60) Gertner, B. J.; Bergsma, J. P.; Wilson, K. R.; Lee, S.; Hynes, J. T. *J. Chem. Phys.* **1987**, *86*, 1377.
- (61) Marcus, R. A. *J. Chem. Phys.* **2006**, *125*, 194504–1.
- (62) Villa, J.; Warshel, A. *J. Phys. Chem. B* **2001**, *105*, 7887.
- (63) Schmitt, U. W.; Voth, G. A. *J. Phys. Chem. B* **1998**, *102*, 5547.